

# Cloud Resolving Model Radar Simulator (CR-SIM)

## 1 An application within the SOS Chuva project

The event considered in this case study (Dezember 3rd, 2016) was configured a result of a trough in higher levels and the South American Low Level Jet transporting humidity in low levels to the region of study. During the event, strong gust winds and/or hail were reported in cities near Piracicaba, as well as in Jundiaí and Campinas.

The case was run with WRF using Morrison Scheme (MP=10) for a 308 x 279 grid with 1 km horizontal resolution and 54 vertical sigma levels, initiated at 1800 UTC. The CRSIM was executed for the time steps corresponding to 1900, 2000 and 2100 UTC, respectively. As illustration, results for 2100 UTC are presented below.

Figure 1 shows the GOES-13 satellite highlighted IR (a), the CAPPI at 3km from the Campinas X-band radar (b) and the CAPPI at 3km from CRSIM results for the same radar (c). A comparison between horizontal reflectivity values from the radar and from CRSIM at this hour is not recommended since the horizontal reflectivity from the radar at this time is likely to be underestimated due to the rain at Campinas, and future simulations that will start earlier to simulate the system as it approaches the radar location are been prepared. Therefore, the analysis conducted aimed to assess whether CRSIM results for polarimetric variables were consistent with the different hydrometeor mixing ratios, according to the characteristics know for the region of study. Vertical profiles of the different hydrometeors and polarimetric variables were also obtained for the four points indicated in 1 (bottom).

For point 1, located in a cell with high horizontal reflectivity ( $> 58$  dBZ at  $15^\circ\text{C}$ ) outside the radar range, results from WRF (hydrometeors mixing ratios) and CRSIM (polarimetric variables) are shown in Figure 2. It can be seen that for this point the model indicated a large quantity of graupel (very likely overestimated) for all temperatures below  $0^\circ\text{C}$ , being larger between  $-10^\circ\text{C}$  and  $-60^\circ\text{C}$  (between 3 and 6 g/kg), while rain is moderately large (up to 7 g/kg) above  $0^\circ\text{C}$ . Other hydrometeor species are present in lesser, but still relevant quantities ( $< 2$  g/kg). The horizontal reflectivity  $Z_H$  is large ( $< 25$  dBZ) for the entire column. Meanwhile,  $Z_{DR}$  and  $K_{DP}$  are larger for the warm layers above  $0^\circ\text{C}$  but almost zero for the colder temperatures between  $0^\circ\text{C}$  and  $-40^\circ\text{C}$  (where, typically, the mixed layer is located). In particular, the value of  $K_{DP}$  is large ( $> 10$   $^\circ/\text{km}$ ) for the warm layer. For the glaciated layer  $Z_{DR}$  continues to be near zero and  $K_{DP}$  has positive values but lower than  $2$   $^\circ/\text{km}$ .

For point 2 (Figure 3), located within the range of the radar in a point with lower  $Z_H$  than point 1 ( $\approx 50$ dBZ at  $15^\circ\text{C}$ ), the graupel and rain mixing ratios are much lower (with maximum at 4 g/kg and 2 g/kg,

respectively, while the maximum mixing ratio for snow is slightly higher (2 g/k) than for point 1 and cloud and ice are almost zero.  $Z_H$  is lower than for point 1, and values are higher than zero in the warm and mixed layers, being below zero for the glaciated layer. The profile of  $Z_{DR}$  is similar than the obtained for point 1 except for the higher values (up to 2.5 dB) at very cold temperatures (below -60°C). The  $K_{DP}$  value is much lower than the obtained for point 1 in the warm layer, and the higher values obtained in the glaciated layer for point 1 are no longer observed.

The point 3 (Figure 4) is located within the range of the radar, with  $Z_H \approx 50$  dBZ at 15 °C) This point exhibits a profile of  $Z_H$  somewhat similar to that of point 2 for the warm layer and most of the mixed layer, with a higher  $Z_H$  in the glaciated layer. Rain and graupel are lower in this case than for points 1 and 2 but the snow profile presents higher values than for those previous cases.  $Z_{DR}$  and  $K_{DP}$  are similar in shape to those obtained for point 2. Cloud and ice are also very low for this case.

Finally, point 4 (Figure 5), also located within the range of the radar, shows a large  $Z_H$  value in the warm layer ( $\approx 55$  dBZ at 15 °C), similar to that of point 1. The  $Z_H$  profile at point 4 is very similar to that obtained for point 1 for the warm and mixed layers, being below zero for the glaciated layer, where all hydrometeors mixing ratio are close to zero. The graupel mixing ratio for this case was higher (with a maximum of  $\approx 5$  g/kg approximately at -30 °C).  $Z_{DR}$  and  $K_{DP}$  profiles are also very similar in shape and magnitude to those obtained for point 1 for the warm and mixed layers, with the  $K_{DP}$  being lower (with a maximum of 9 °/km).

## 2 Results with Thompson micro-physic scheme

The same case study was run with the same configuration of WRF, but using Thompson micro-physic scheme. The horizontal reflectivity at the same hour (2000 UTC) is presented in Figure 6. It can be seen that in this case the reflectivity values are in general lower than those obtained with the Morrison micro-physic scheme, although a line with high convection values around 47 degrees west is still evidenced. Due to the differences in the reflectivity pattern, the positions of the profiles of hydrometeor mixing ratios and polarimetric variables were different in order to select areas with high convection.

In this case, the point 1 is also located in a cell with high horizontal reflectivity ( $\approx 50$  dBZ at 15 °C) outside the radar range, results from WRF (hydrometeors mixing ratios and horizontal reflectivity) are shown in Figure 2. It can be seen that for this point the model indicated a larger quantity of snow (maximum of 3 g/kg at -40 °C) than of cloud droplets (maximum of  $\approx 2$  at -10 °C) and of graupel (two maximums of  $\approx 1.5$  g/kg at -5 and -30 °C), while rain is moderately large (up to 5 g/kg) above -5 °C and ice mixing ratio is very low. The horizontal reflectivity  $Z_H$  is large ( $< 30$  dBZ) for the warm and mixed layer, and decrease from 20 dBZ to below zero values in the glaciated layer. Local maximum of reflectivity take place at approximately the same temperature that the graupel maximums.

The point 2 (Figure 8) presents a lower reflectivity than point 1 at 15 °C but a higher value at the melting point of 60 dBZ. As for point 1, the snow mixing ratio is higher than the mixing ratio of other species, reaching a maximum of 4 g/kg. The maximum of reflectivity also take place at approximately the same

temperature that the graupel maximums.

For point 3, the reflectivity profile is similar to the obtained for point 2 for the warm and mixed layer, but lower for the glaciated layer, decreasing to zero at  $-50\text{ }^{\circ}\text{C}$ . In this case, mixing ratios of rain droplets, cloud droplets, graupel and snow present maximum between 1.5 and 2 g/kg at different heights.

Finally, the reflectivity at point 4 (Figure 8) is also high in the warm layer but decrease to values below 0 dBZ at approximately  $-30\text{ }^{\circ}\text{C}$ . Cloud droplets, rain droplets and graupel mixing ratios present maximum of about 3 g/kg, while snow and ice are close to zero.

### 3 Conclusions

Although the WRF output for hydrometeors appears to be overestimated for the Morrison scheme (in particular, graupel values seems too large), the output from CRSIM appears to be, in general, consistent with WRF results, considering the considerations considered within CRSIM. In particular, the selected considerations for shape in the LUT appears to influence results in a significant way.

For this particular case, results obtained using Thompson scheme seem to be relatively more consistent with the micro-physics of cloud development than those obtained with Morrison, both in terms of the mixing ratio relative values and temperature at which maximum take place.

Some general questions arrived from the study of the documentation and after the use of CRSIM for this case study. These questions, detailed below, also consider the area of study and the intended use of CRSIM within the model.

### 4 General questions:

- It would be possible to include the correlation coefficient? This would be a very useful addition to the set of polarimetric variables already available, and CRSIM already has all parameters needed to estimate this variable.
- What would be the procedure to include Thompson micro-physics scheme (or other scheme) in CRSIM?
- According to the look-up table (LUT) for scattering types in slide 3 in `crm_radar_simulator.pptx` document, the shape of all hydrometeors is considered to be oblate, with their longer dimension in the horizontal plane. Is this interpretation correct? In this case:
  - How is it possible to obtain negative values for  $K_{DP}$  (slide 5, same document)
  - It would be possible to include vertically oriented ice or graupel? A previous study in the same region covered by SOS the Chuva experiment showed that high lightning activity (commonly observed during the wet season in this region) is frequently associated with regions of negative  $Z_{DR}$  and  $K_{DP}$  with moderate  $Z_H$ , most likely due to the presence of conical graupel oriented vertically due to the electrical field (Mattos et al. 2016).

- Also in the LUT presented in slide 3 in `crm_radar_simulator.pptx` document, it can be seen that only cloud and rain have values for a temperature range, while ice, snow and graupel are cited to be values only for a  $-20\text{ }^{\circ}\text{C}$  temperature. Does this mean that no other possible temperature values are considered for these species? Is this the same as assuming that temperature do not influence the polarimetric signatures of these species?

## References

Mattos, Enrique V et al. (2016). “Polarimetric radar characteristics of storms with and without lightning activity”. In: *Journal of Geophysical Research: Atmospheres* 121.23.

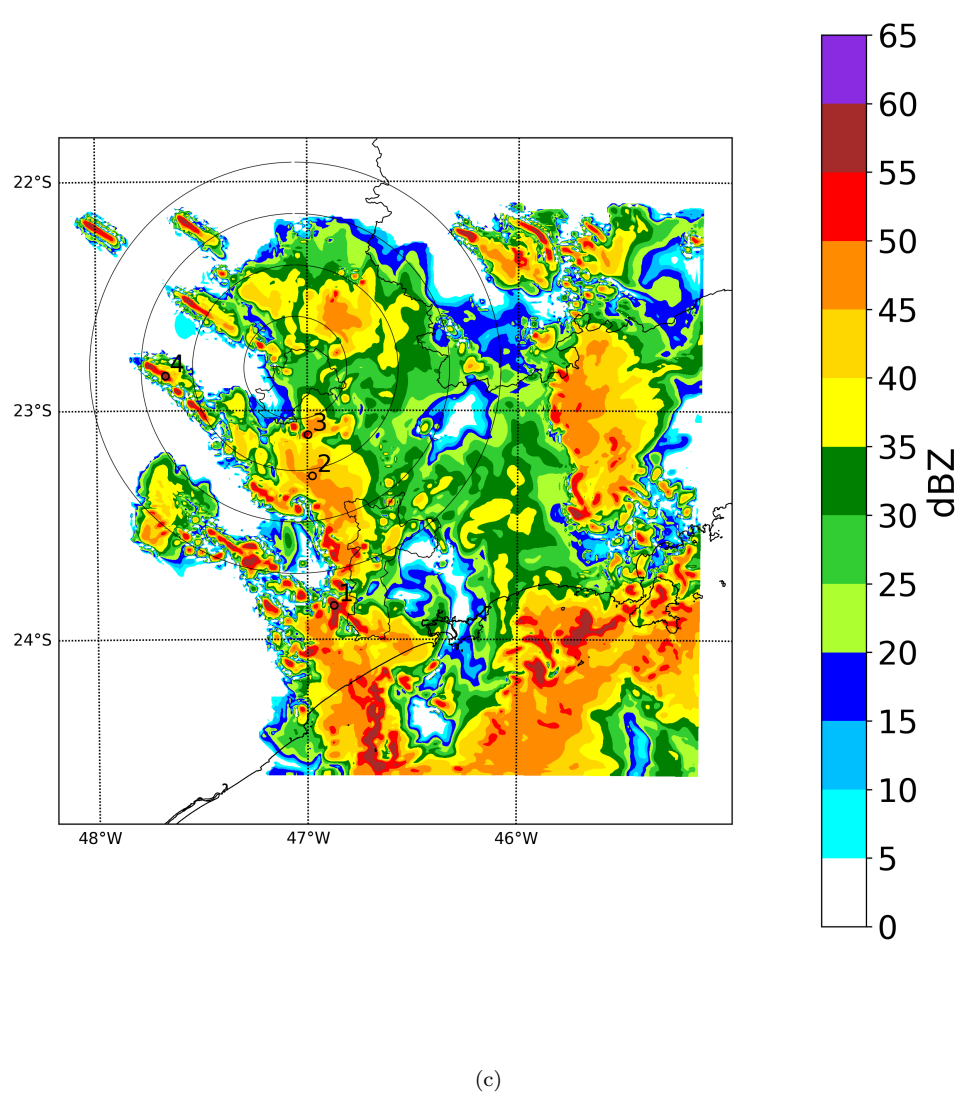
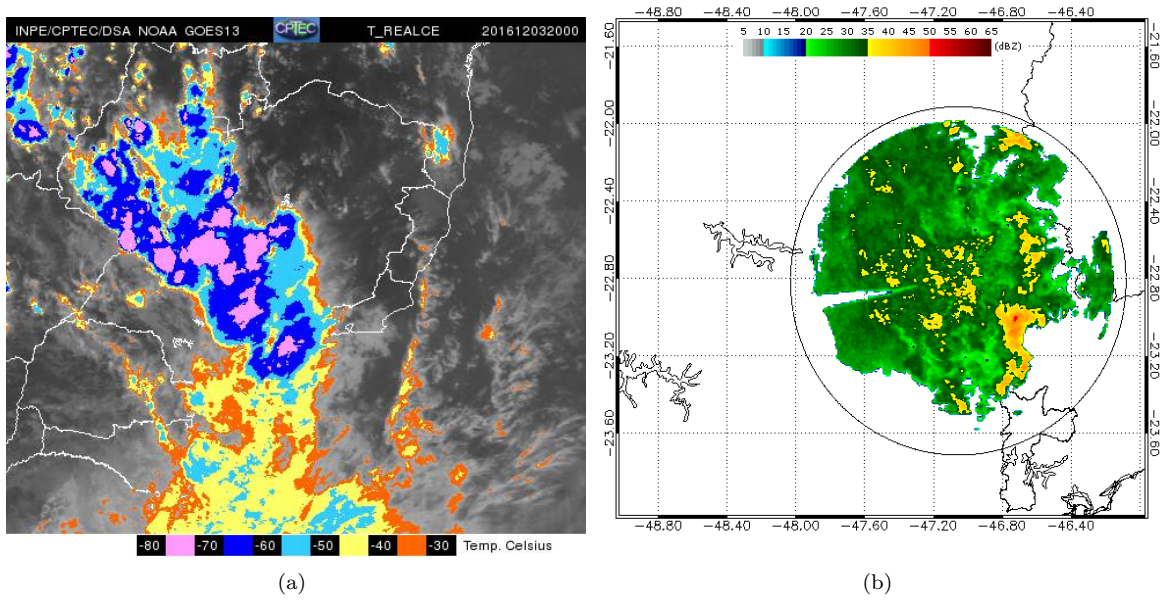


Figure 1: a) GOES-13 highlighted IR, b) Reflectivity from X-band radar at Campinas and c) CRSIM derived reflectivity from WRF run, at 2000 UTC. Points used for vertical profiles are indicated.

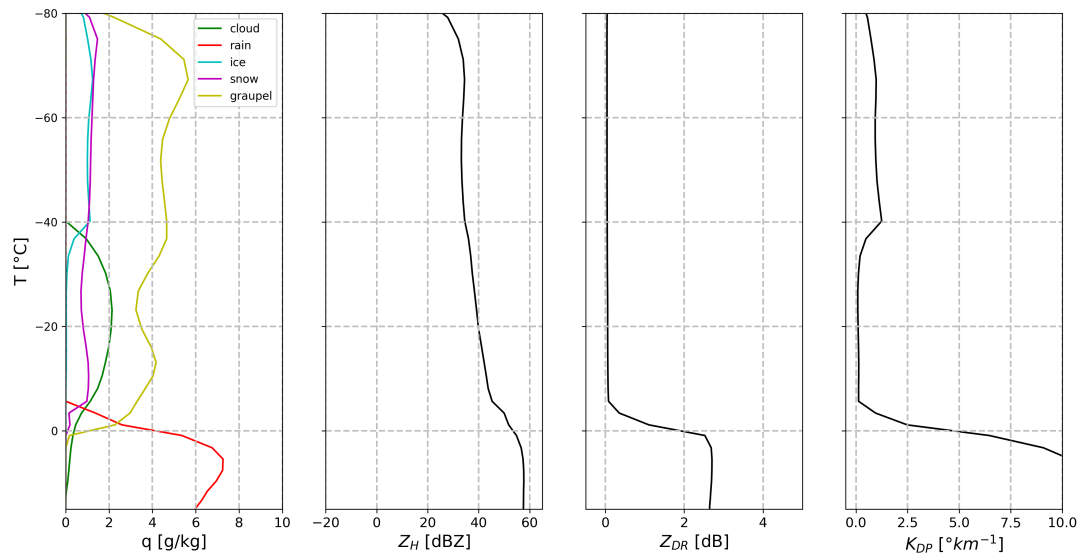


Figure 2: Hydrometeors mixing ratios and polarimetric variables for point 1.

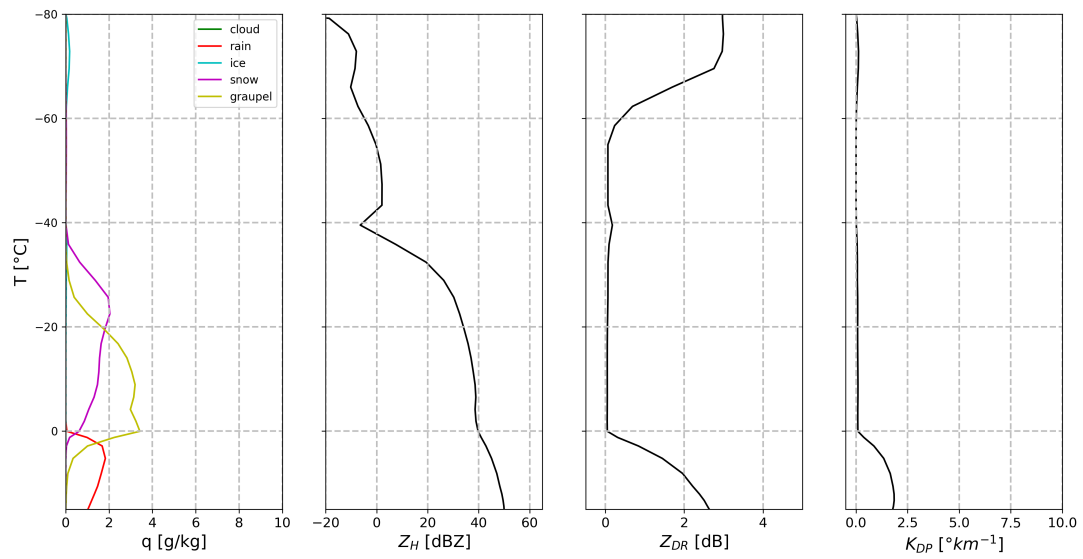


Figure 3: Hydrometeors mixing ratios and polarimetric variables for point 2.

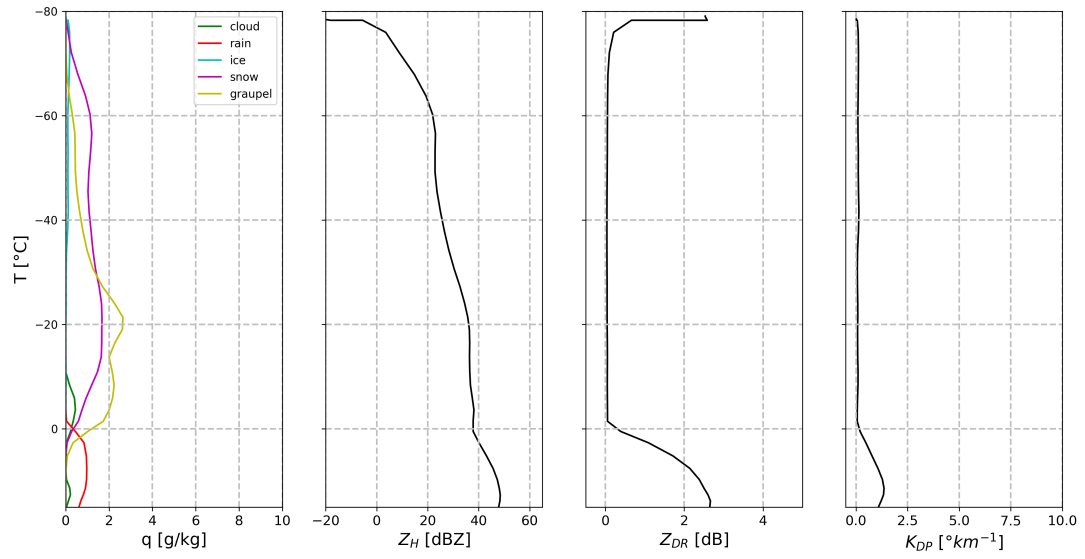


Figure 4: Hydrometeors mixing ratios and polarimetric variables for point 3.

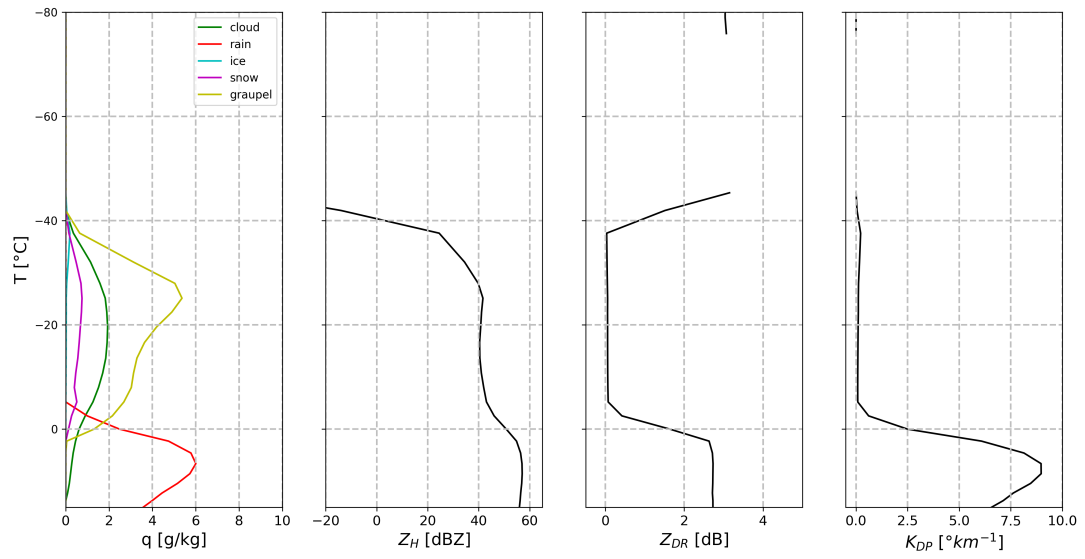


Figure 5: Hydrometeors mixing ratios and polarimetric variables for point 4.

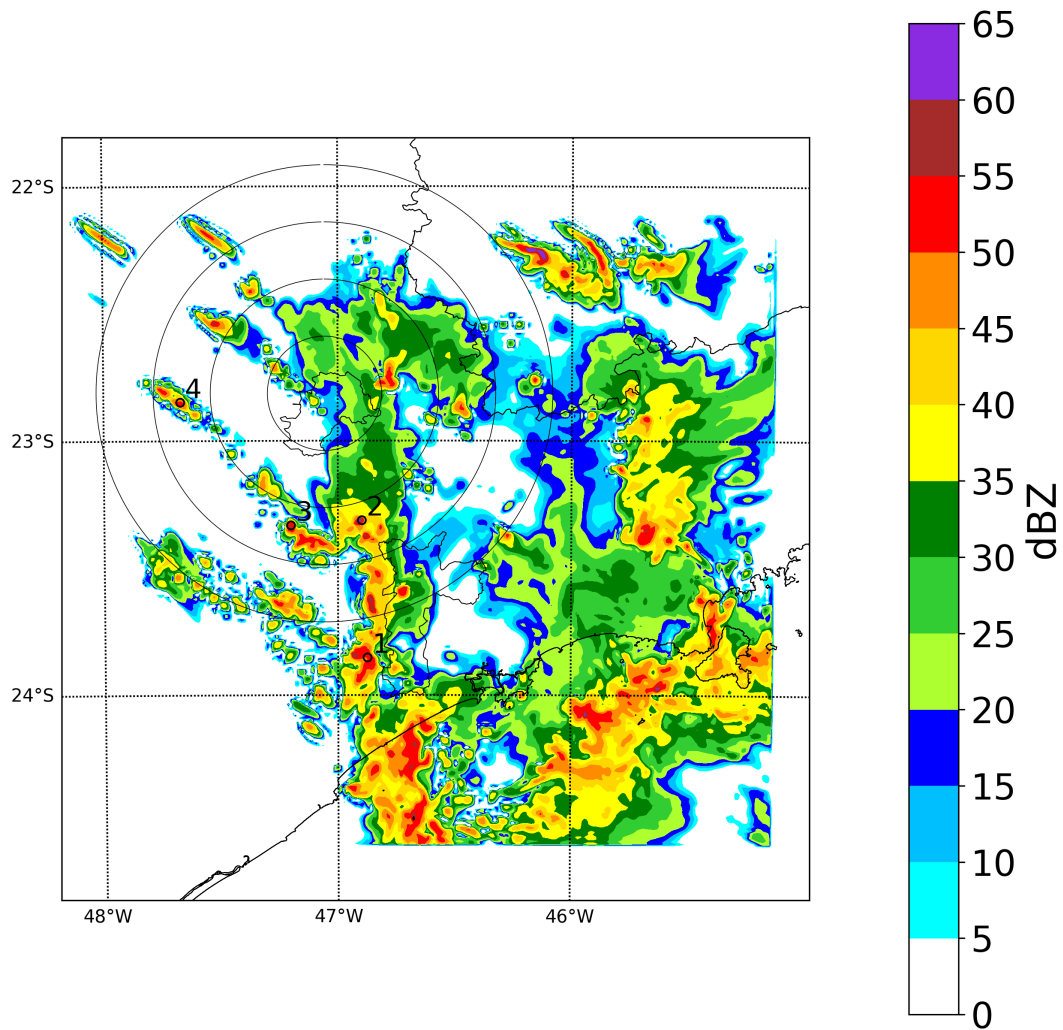


Figure 6: Horizontal reflectivity at 3 km obtained with WRF using Thompson micro-physic scheme, at 2000 UTC. Points used for vertical profiles are indicated.

### Mixing ratios for point 1 lat:-23.8524 lon -46.8735

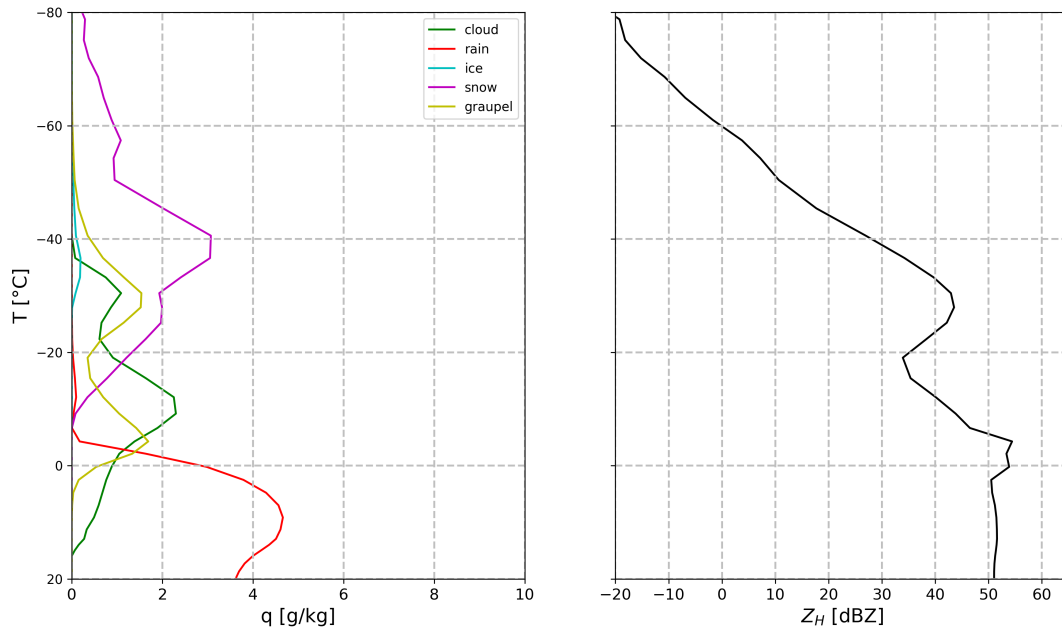


Figure 7: Hydrometeors mixing ratios and horizontal reflectivity for point 1, Morrison micro-physic scheme.

### Mixing ratios for point 2 lat:-23.3129 lon -46.8973

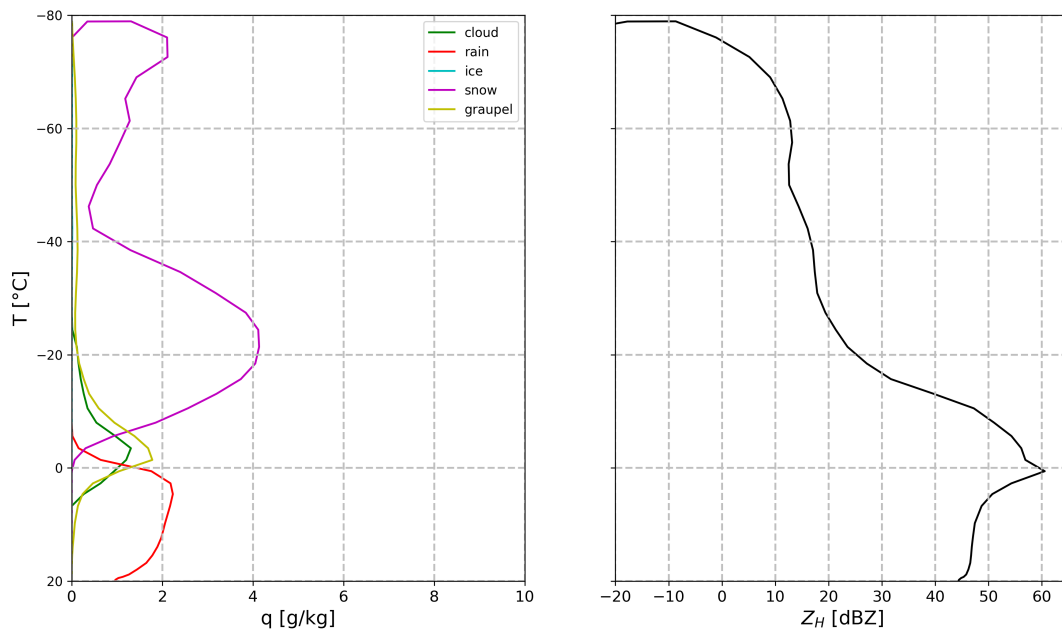


Figure 8: Hydrometeors mixing ratios aand horizontal reflectivity for point 2, Morrison micro-physic scheme.

### Mixing ratios for point 3 lat:-23.3326 lon -47.2008

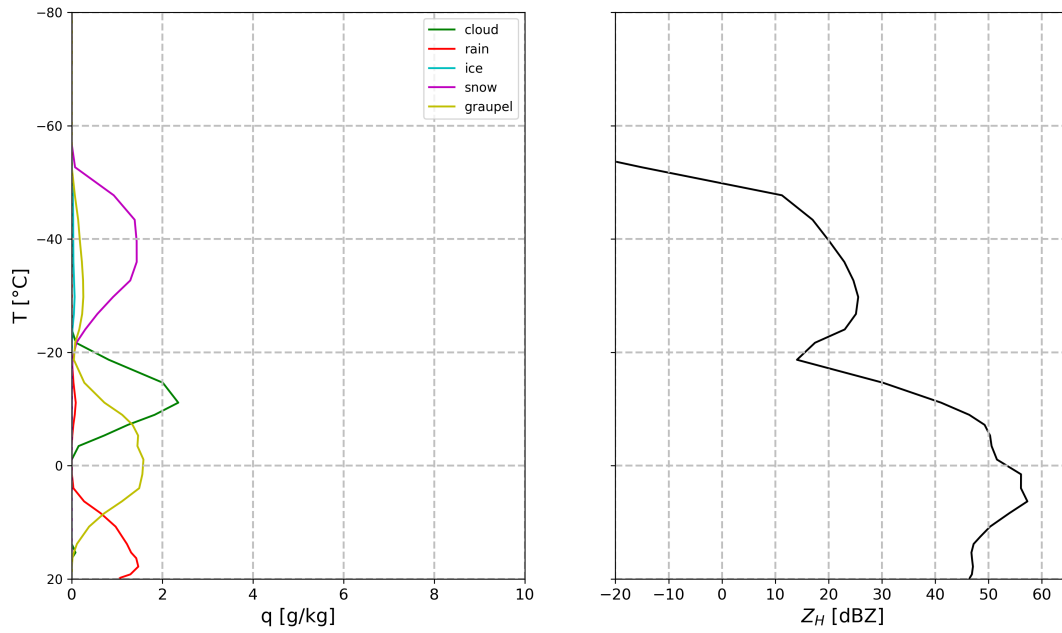


Figure 9: Hydrometeors mixing ratios and horizontal reflectivity for point 3, Morrison micro-physic scheme.

### Mixing ratios for point 4 lat:-22.8483 lon -47.6719

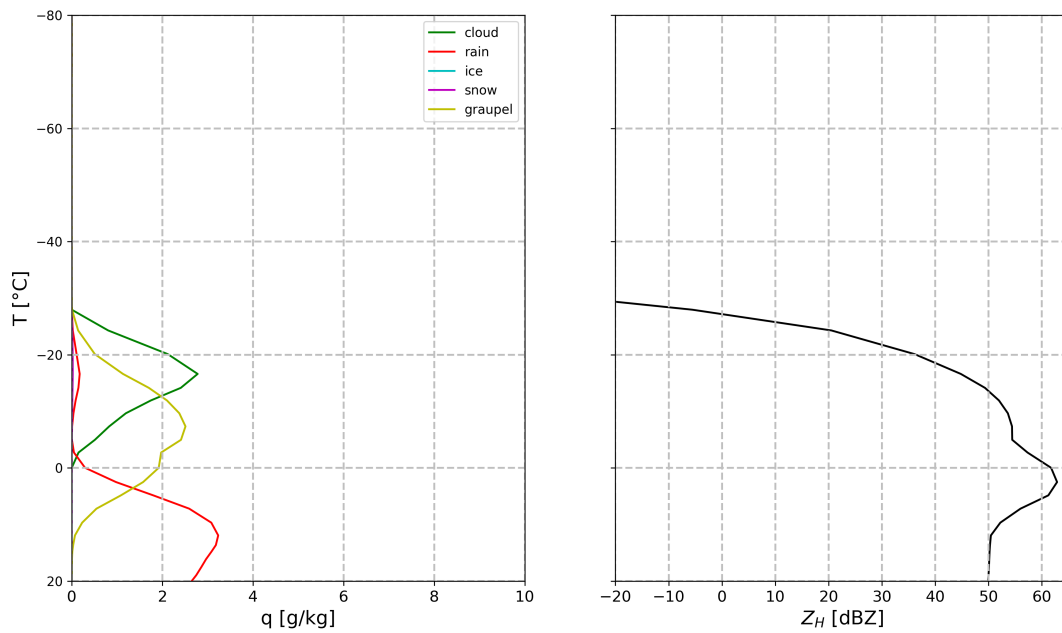


Figure 10: Hydrometeors mixing ratios and horizontal reflectivity for point 4, Morrison micro-physic scheme.